Rationalization of Enantioselectivities in Dialkylzinc Additions to Benzaldehyde Catalyzed by Fenchone Derivatives†

Bernd Goldfuss,*,‡ Melanie Steigelmann,‡ Saeed I. Khan,§,|| and K. N. Houk§

Organisch-Chemisches Institut der Universität Heidelberg, Im Neuenheimer Feld 270, D-69120 Heidelberg, Germany, and Department of Chemistry and Biochemistry, University of California, Los Angeles 405 Hilgard Avenue, Los Angeles, California 90095-1569

Received July 6, 1999

Three (−)-fenchyl alcohol derivatives, {(1*R*,2*R*,4*S*)-*exo*-(2-Ar)-1,3,3-trimethylbicyclo[2.2.1] heptan-2-ol, Ar = *o*-anisyl (**2**), 2-*N*-methylimidazolyl (**3**), 2-*N*,*N*-dimethylbenzylamine (**4**)} were synthesized, characterized by X-ray analyses, and employed as precatalysts in diethyl zinc additions to benzaldehyde. Directions and relative degrees of enantioselectivities are rationalized by QM/MM ONIOM computations of μ-O transition structure models. Enantioselectivities arise from repulsive interactions between "transferring" or "passive" alkyl groups at the zinc centers and the substituents at donor groups or the bicyclo[2.2.1]heptane moieties. These results enable predictions for ligand-tuning to improve catalyst efficiency of fenchone-based ligands in dialkylzinc additions to aldehydes.

Introduction

Enantioselective 1,2-additions of organometallic reagents to prochiral carbonyl compounds are fundamental in syntheses of optically active molecules.[1] Hence, the design of efficient chiral promoters for these processes is of central interest.[2] Combinatorial methods for syntheses and high throughput screening of catalysts are being developed currently[3] but hardly provide answers for the puzzling questions regarding the *origins* of enantioselectivities. This knowledge, however, is essential for a *rational* catalyst design.

Noyori et al. reported profound experimental[4] and computational[5] studies of (2*S*)-3-*exo*-(dimethylamino)-isoborneol (DAIB) catalyzed dialkylzinc, ZnR_2 (R = Me, Et), additions to benzaldehyde. The enantioselective step was found to proceed through "anti" and "syn" μ-O transition structures.[5] We have recently shown that μ-O transition structure models can be successfully employed to understand enantioselectivities with other chiral β-amino alcohols, e.g., proline and 1,2-diphenylethane derivatives.[6]

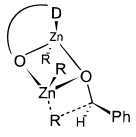

anti μ-O TS

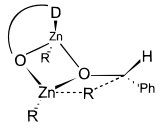

syn μ-O TS

A large number of chiral chelating ligands has been synthesized and applied in enantioselective additions of organozincs[7] to aldehydes,[2,8] but ligands with short synthetic routes are still desirable. Additions of donor-functionalized organolithiums to fenchone provide efficient one-step routes to chiral chelating fenchyl alcohol ligands (e.g. **1**). For **1**, however, only moderate enantioselectivities were reported (64% ee of (*R*)-1-phenylpropanol).[9]

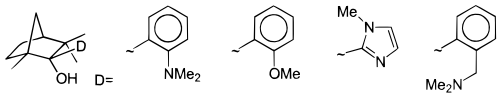

1 **2** **3** **4**

To explore origins of the enantioselectivities, we synthesized fenchone-based ligands with different coordination groups (D), **2**−**4**, and employed them as precatalysts in dialkylzinc additions to benzaldehyde. The stereo-

† This article is dedicated to Prof. Paul von Ragué Schleyer on the occasion of his 70th birthday.

* Corresponding author. E-mail: Bernd.Goldfuss@urz.uni-heidelberg.de.

‡ Organisch-Chemisches Institut der Universität Heidelberg.

§ Department of Chemistry and Biochemistry, UCLA.

|| Responsible for X-ray crystal analysis.

(1) (a) Helmchen, G.; Hoffmann, R. W.; Mulzer, J.; Schaumann, E., Eds. *Methods of Organic Chemistry* (Houben Weyl); Thieme: Stuttgart, 1996; Vol. E21b. (b) Thompson, A.; Corley, E. G.; Huntington, M. F.; Grabowski, E. J. J.; Remenar, J. F.; Collum, D. B. *J. Am. Chem. Soc.* **1998**, *120*, 2028. (c) Pierce, M. E.; Parsons, R. L., Jr.; Radesca, L. A.; Lo, Y. S.; Silverman, S.; Moore, J. R.; Islam, Q.; Choudhury, A.; Fortunak, J. M. D.; Nguyen, D.; Luo, C.; Morgan, S. J.; Davis, W. P.; Confalone, P. N.; Chen, C.; Tillyer, R. D.; Frey, L.; Tan, L.; Xu, F.; Zhao, D.; Thompson, A. S.; Corley, E. G.; Grabowski, E. J. J.; Reamer, R.; Reider, P. J. *J. Org. Chem.* **1998**, *63*, 8536.

(2) (a) Soai, K.; Niwa, S. *Chem. Rev.* **1992**, *92*, 833. (b) Noyori, R.; Kitamura, M. *Angew. Chem.* **1991**, *103*, 34; *Angew. Chem., Int. Ed. Engl.* **1991**, *30*, 49. (c) Evans, D. A. *Science* **1998**, *22*, 420.

(3) Enantioselective diethylzinc additions to benzaldehyde: (a) Ding K.; Ishii, A.; Mikami, K. *Angew. Chem.* **1999**, *111*, 519; *Angew. Chem., Int. Ed.* **1999**, *38*, 497. (b) Gennari, C.; Ceccarelli, S.; Piarulli, U.; Montalbetti, C. A. G. N.; Jackson, R. F. *J. Org. Chem.* **1998**, *63*, 5312. (c) Liu, G.; Ellman, J. A. *J. Org. Chem.* **1995**, *60*, 7712. Epoxidations: (d) Francis, M. B.; Jacobsen, E. N. *Angew. Chem.* **1999**, *111*, 987; *Angew. Chem., Int. Ed.* **1999**, *38*, 937. Strecker reactions: (e) Sigman, M. S.; Jacobsen, E. N. *J. Am. Chem. Soc.* **1998**, *120*, 4901. Screening: (f) Bein, T. *Angew. Chem.* **1999**, *111*, 335, *Angew. Chem., Int. Ed.* **1999**, *38*, 323. (g) Kagan, H. B. *J. Organomet. Chem.* **1998**, *567*, 3. (h) Shimizu, K. D.; Snapper, M. L.; Hoveyda, A. H. *Chem. Eur. J.* **1998**, *4*, 1885.

(4) (a) Kitamura, M.; Okada, S.; Suga, S.; Noyori, R. *J. Am. Chem. Soc.* **1989**, *111*, 4028. (b) Kitamura, M.; Suga, S.; Kawai, K.; Noyori, R. *J. Am. Chem. Soc.* **1986**, *108*, 6071.

(5) (a) Yamakawa, M.; Noyori, R. *Organometallics* **1999**, *18*, 128. (b) Yamakawa, M.; Noyori, R. *J. Am. Chem. Soc.* **1995**, *117*, 6327.

(6) Goldfuss, B.; Houk, K. N. *H. J. Org. Chem.* **1998**, *63*, 8998.

(7) (a) Knochel, P.; Langer, F.; Longeneau, A.; Rottländer, M. Stüdemann, T. *Chem. Ber./Recueil* **1997**, *130*, 1021. (b) Knochel, P.; Singer, R. D. *Chem. Rev.* **1993**, *93*, 2117.

(8) Ferrocenyl hydroxy oxazolines: (a) Bolm, C.; Muniz, K. *Chem. Commun.* **1999**, 1295. (b) Bolm, C.; Muniz-Fernandez, K.; Seger, A.; Raabe, G.; Günther, K. *J. Org. Chem.* **1998**, *63*, 7860. Arene chromium ligands: (c) Bolm. C.; Muniz, K. *Chem. Soc. Rev.* **1999**, *28*, 51. Titanium TADDOLates: (d) Weber, B.; Seebach, D. *Tetrahedron* **1994**, *50*, 7473. (e) Schmidt, B.; Seebach, D. *Angew. Chem.* **1991**, *103*, 1383; *Angew. Chem., Int Ed. Engl.* **1991**, *30*, 99.

10.1021/jo991070v CCC: $19.00
Published on Web 12/17/1999

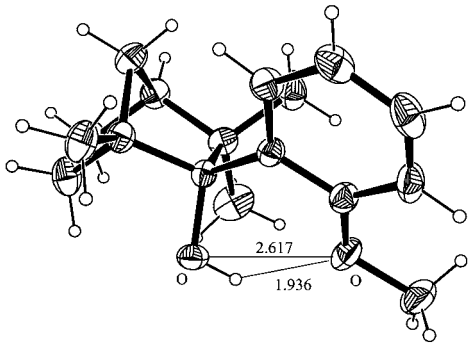

2

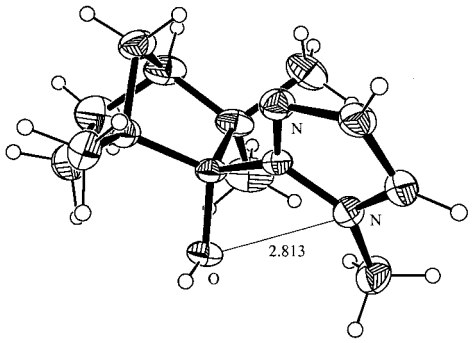

3

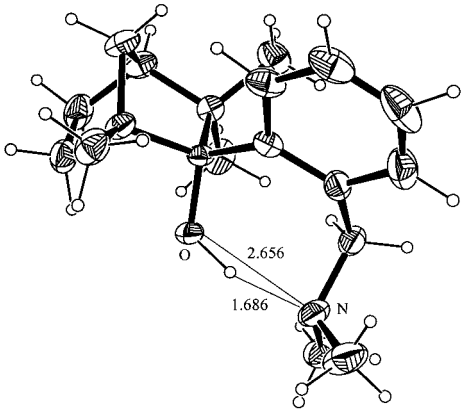

4

Figure 1. X-ray crystal structures of **2**−**4**.[20] Distances are given in angstroms.

chemical outcome of these reactions was rationalized by transition structure modeling. The effects of different coordination groups on the enantioselectivities were analyzed. With these studies we intend to provide a basis for rational catalyst design.

Table 1. Enantioselective Additions of Diethylzinc to Benzaldehyde

ligand	T	reaction time (h)	chemical yield (%)	enantiomer[d]	%op[e]	%ee[f]
1[a]	rt	24	99	*R*	64	−
2[b]	−30 °C	24	56[c]	*S*	24	26
3[b]	+6 °C	24	71[c]	*S*	35	37
4[b]	+6 °C	24	57[c]	*S*	72	73

[a] In toluene/hexanes, 3 mol % ligand; see ref 9. [b] In hexanes, 3 mol % ligand. [c] GC analysis. [d] Major enantiomer of the 1-phenyl-1-propanol product. [e] Optical purity. [f] Enantiomeric excess, chiral HPLC analysis.

Results and Discussion

Synthesis and Structural Characterization of the Ligands. To evaluate the effects of catalyst structure on enantioselectivities with fenchone-based ligands, we synthesized three chelating fenchyl alcohols with different coordination functions D, **2** (D = C_6H_4OMe), **3** (D = $C_3H_2N_2Me$), and **4** (D = $C_7H_6NMe_2$).

X-ray crystal analyses of these ligands reveal hydrogen-bonding between the hydroxy functions and the donor atoms O and N for **2** and **4**, but not for **3** (Figure 1). The imino nitrogen atom of the imidazolyl moiety in **3** is oriented toward the $-CH_2-$ bridge of the bicyclo[2.2.1]-heptane skeleton rather than to the hydroxy group (Figure 1). However, chelation of zinc centers requires syn alignment of imino nitrogen and oxygen atoms, as is apparent in the transition structure models (see below).[10] The aromatic ring systems of the D-functions are not aligned coplanar with the C−O(H) bonds but are tilted by 47.2° (**2**), 35.5° (**3**), and 42.7° (**4**). The high degree of substitution and the eclipsed arrangement in the bicyclo-[2.2.1]heptane moiety results in long C_2-C_3 bonds: 1.61 Å (**2**), 1.57 Å (**3**), and 1.61 Å (**4**). We have recently reported X-ray crystal structures of complexes of ligand **2** with *n*-butyllithium and methylzinc.[11]

Experimental Observations and Computational Rationalizations. The performances of ligands **1**,[9] **2**, **3**, and **4** as promoters in enantioselective diethylzinc additions to benzaldehyde are summarized in Table 1. Despite the structural similarity to **1**, which produces (*R*)-1-phenyl-1-propanol, ligands **2**−**4** all yield (*S*)-1-phenyl-1-propanol as major enantiomer. The highest enantiomeric excess of (*S*)-1-phenyl-1-propanol is produced by ligand **4**.

Why does ligand **1** give (*R*)-1-phenyl-1-propanol, while **2**−**4** all produce the *S*-enantiomer as the major product? PM3 μ-O transition structure models, which proved successful for some β-amino alcohols,[6] were also applied for ligands **1**−**4**. Only poor agreement with the experimental enantioselectivities was obtained. A reason for

Table 2. Computed (RHF/LanL2DZ:UFF) Total (au) and Relative (kcal/mol) Energies of μ-O Syn and Anti Transition Structures[a]

	anti(*R*) (ZPE)[b]	anti(*S*) (ZPE)[b]	syn(*R*) (ZPE)[b]	syn(*S*) (ZPE)[b]
1	−434.90794 (427.0)	−434.88323 (426.5)	−434.88777 (427.0)	−434.90292 (427.6)
rel	0.0	15.5 (15.0)	12.7 (12.7)	3.2 (3.8)
2	−434.91175 (398.5)	−434.89675 (398.9)	−434.88393 (397.9)	−434.91230 (398.9)
rel	0.3 (−0.1)	9.8 (9.8)	17.8 (16.8)	0.0
3	−434.85744 (375.4)	−434.84132 (375.8)	−434.83510 (376.5)	−434.86241 (375.9)
rel	3.1 (2.6)	13.2 (13.1)	17.1 (17.7)	0.0
4	−434.89222 (447.0)	−434.89707 (446.4)	−434.89304 (446.9)	−434.88370 (447.0)
rel	3.0 (3.6)	0.0	2.5 (3.0)	8.4 (9.0)

[a] "Anti" and "syn" denote the types of the transition structures and (*R*) and (*S*) show the configurations of the products. Transition structure optimizations and frequency analyses were performed by ONIOM (RHF/LanL2DZ:UFF) computations. A single imaginary frequency corresponds in all cases to methyl transfer from zinc to the aldehyde carbon atom. [b] Zero point energies (ZPE, kcal/mol) and relative energies with ZPE correction are given in parentheses.

the deviation from experimental results is seen in the strong overestimation of "agostic" interactions between zinc ions and alkyl groups of the ligands by the PM3 method.[12] We hence explored a combined ab initio/molecular mechanics approach[13] to model μ-O anti and syn transition structures.

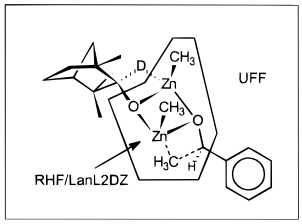

The inner cores of the transition structures were optimized ab initio (RHF/LanL2DZ), while Rappe's universal force field (UFF)[14] was employed for the ligands and the phenyl groups.

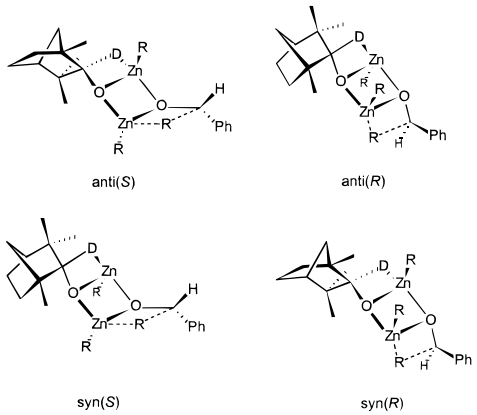

Ethyl groups were replaced by methyl groups to eliminate conformational freedom in the transition structures.[15]

Anti(*R*) and syn(*S*) transition structures are computed most stable for ligands **1**, **2**, and **3**, while anti(*S*) and syn-(*R*) are low-energy transition structures for **4** (Table 2). In agreement with the experimental results (Table 1), **1** yields the *R*-alcohol via **1**-anti(*R*), while **2**−**4** are predicted to generate the *S*-alcohol as the major enantiomer, via **2**-syn(*S*), **3**-syn(*S*), and **4**-anti(*S*) (Table 2).

The reason for the favor of (*R*)-1-phenyl-1-propanol by **1** is shown in Figure 2. The lower stability of "syn" relative to "anti" structures has been attributed to repulsive interactions between alkyl groups on the same side (syn) of the Zn_2O_2 rings.[5,6] This repulsion, however,

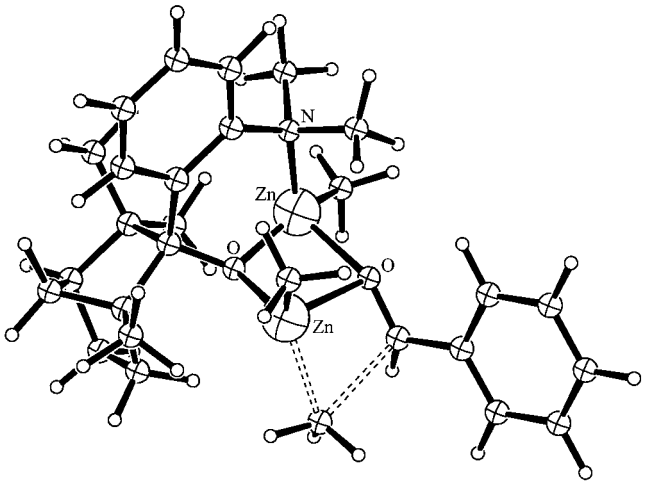

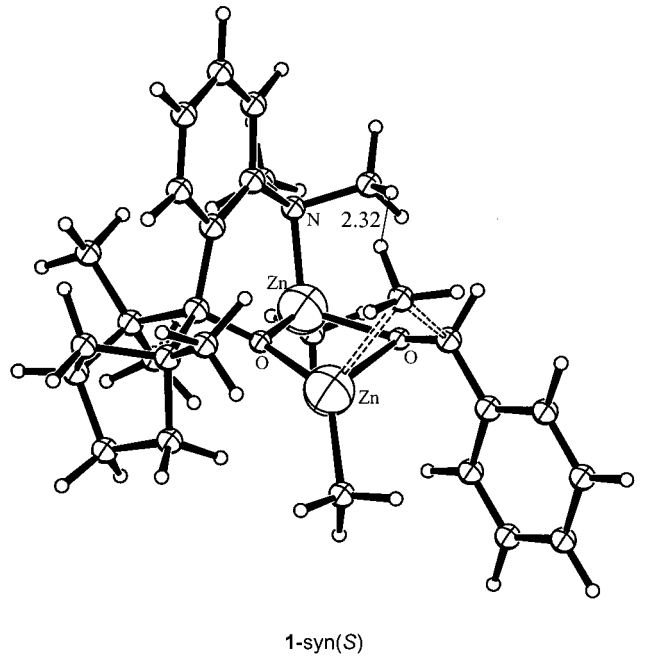

Figure 2. Transition structure geometries of **1**-anti(*R*) and **1**-syn(*S*); ONIOM(RHF/LanL2DZ:UFF). Distances are given in angstroms.

seems not to be significant in **1**-syn(*S*), as the syn alkyl groups are separated by a large distance (>6.0 Å). The lower stability of **1**-syn(*S*) relative to **1**-anti(*R*) obviously arises from close contacts between N−CH_3 groups and the transferring alkyl group R ($H_2CH\cdots HCH_2$, 2.32 Å; Figure 2).[16] For equivalent groups in **1**-anti(*R*), no such unfavorable contacts are apparent ($H_2CH\cdots HCH_2$, >2.8 Å; Figure 2).

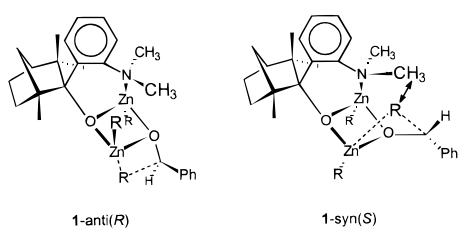

Close contacts as in **1**-syn(*S*) between methylamino and methylzinc groups (Figure 2) do not appear in transition

(9) Genov, M.; Kostova, K.; Dimitrov V. *Tetrahedron: Asymmetry* **1997**, *8*, 1869.

(10) A PM3 conformational analysis shows that repulsion between the *N*-methyl substituent and the −CH_2− bridge of the bicyclo[2.2.1]-heptane skeleton is responsible for this conformation in the X-ray crystal structure of **3**. The X-ray structure of **3** represents the global minimum, but a 2.9 kcal/mol less stable conformer with a syn−periplanar alignment of imino-nitrogen and oxygen atoms was found.

(11) Goldfuss, B.; Khan, S. I.; Houk, K. N. *Organometallics* **1999**, *18*, 2927.

(12) Opitz, A.; Koch, R.; Katritzky, A. R.; Fan, W. Q.; Anders, E. *J. Org. Chem.* **1995**, *60*, 3743.

(13) Dapprich, S.; Komaromi, I.; Byun, K. S.; Morokuma, K.; Frisch, M. J. *Theochem.* **1999**, *461*−*462*, 1.

(14) Rappé, A. K.; Casewit, C. J.; Colwell, K. S.; Goddard III, W. A.; Skiff, W. M. *J. Am. Chem. Soc.* **1992**, *114*, 10024.

(15) The replacement of ethyl by methyl groups is expected to result in no significant errors in comparisons between experiments and computations. Only *relative trends* among the ligands are discussed.

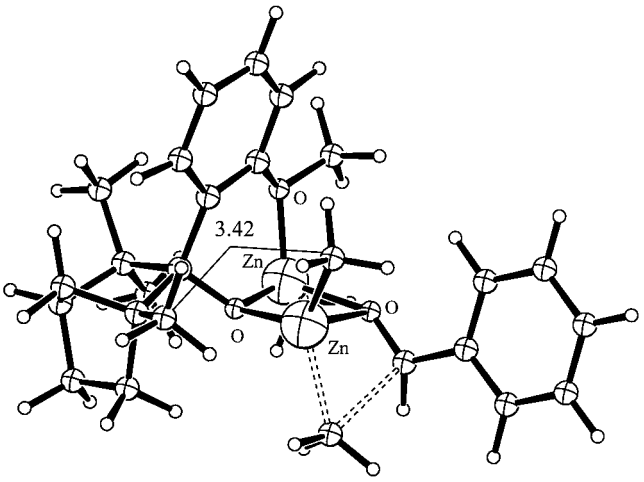

2-anti(*R*)

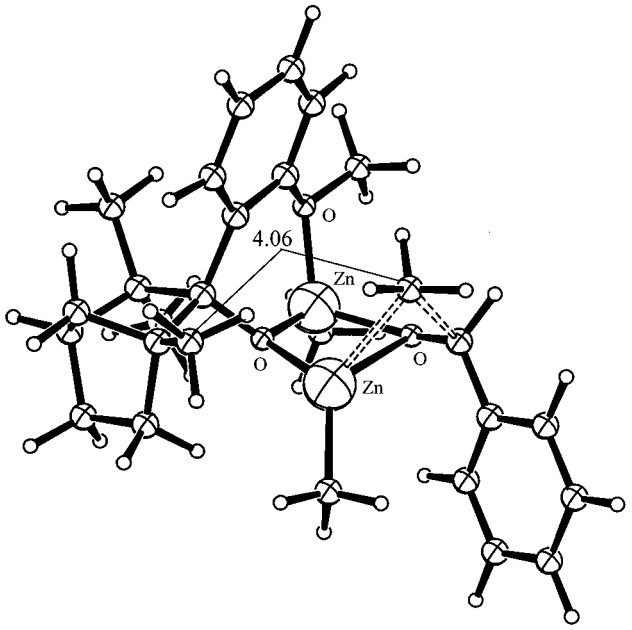

2-syn(*S*)

Figure 3. Transition structure geometries of **2**-anti(*R*) and **2**-syn(*S*); ONIOM(RHF/LanL2DZ:UFF). Distances are given in angstroms.

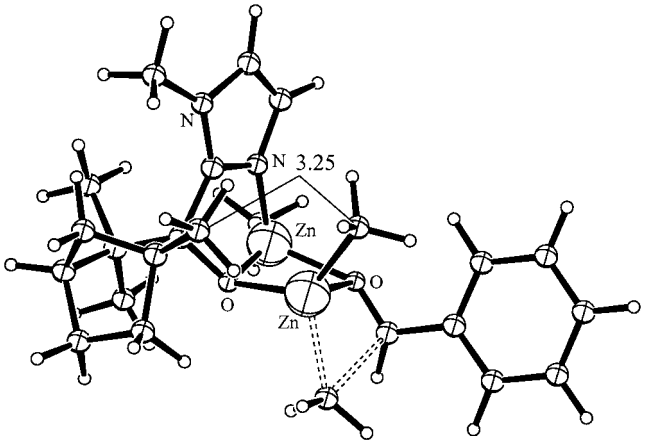

3-anti(*R*)

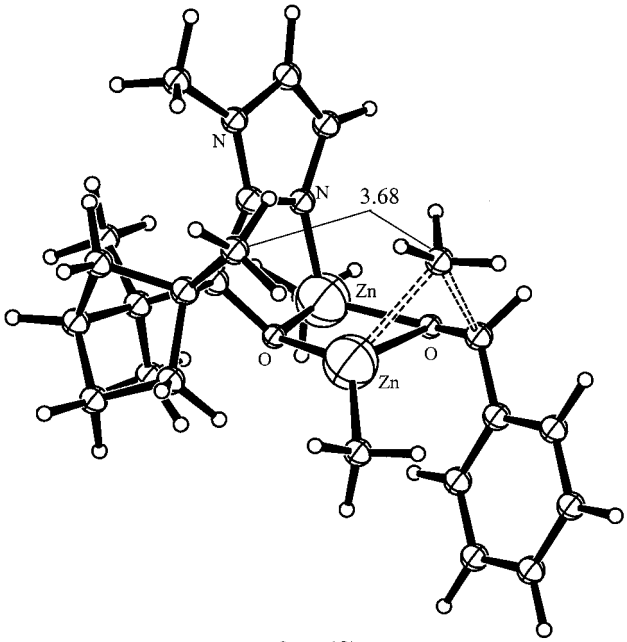

3-syn(*S*)

Figure 4. Transition structure geometries of **3**-anti(*R*) and **3**-syn(*S*); ONIOM(RHF/LanL2DZ:UFF). Distances are given in angstroms.

structures for ligand **2** between methoxy and methylzinc moieties (Figure 3). As a consequence, **2**-anti(*R*) and **2**-syn(*S*) are similar in energy (Table 2) and correspond to low experimental enantioselectivities (Table 1).

Relative to **2**, increased enantioselectivity yielding the *S*-alcohol is observed for ligand **3** experimentally (Table 1) and computationally (Table 2). The preference of the *S*-product for ligands **2** and **3** arises from favored syn(*S*) and disfavored anti(*R*) structures (Table 2). In the disfavored anti(*R*) structures of **2** and **3**, the passive (i.e. not transferring) alkyl groups at zinc and the methyl substituent at C_1 of the bicyclo[2.2.1]heptane moieties exhibit rather close distances (C···C, 3.42 Å in **2**-anti(*R*) and 3.25 Å in **3**-anti(*R*); Figures 3 and 4). However, in the favored syn(*S*) structures of **2** and **3**, this methyl zinc group is transferred to benzaldehyde and is hence aligned in a more remote position. This results, relative to **2**,**3**-anti(*R*), in longer distances between the transferring alkyl groups (R) at zinc and the methyl substituents at C_1 of the bicyclo[2.2.1]heptane moieties in **2**-syn(*S*) (4.06 Å) and in **3**-syn(*S*) (3.68 Å; Figures 3 and 4) and rationalizes the preferred formation of the *S*-alcohol. Relative to **2** (six-membered chelate ring), for ligand **3** (five-membered chelate ring) the C···C distances in anti and syn structures are shorter and the (de)stabilization effects are more intense for **3**. This explains the higher degree of enantioselectivity for **3** relative to **2**.

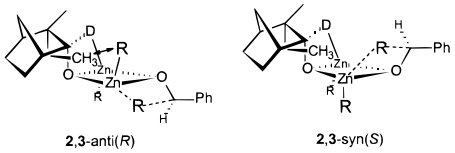

2,**3**-anti(*R*) **2**,**3**-syn(*S*)

For ligand **4**, anti(*S*) and syn(*R*) are the most stable transition structures (Table 2, Figure 5). Close contacts

(16) 2.4 Å is frequently discussed as the van der Waals radius for H atoms, e.g. ref 5a.

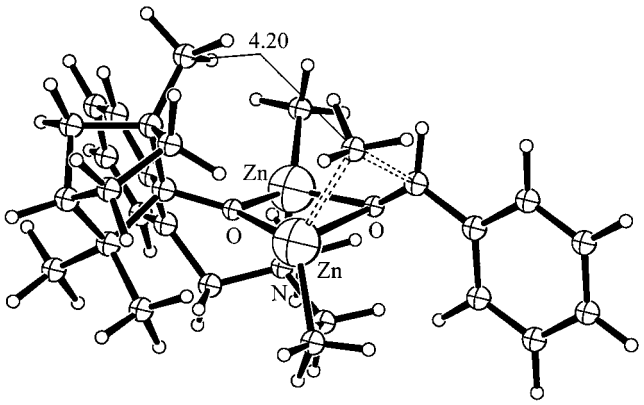

4-anti(*S*)

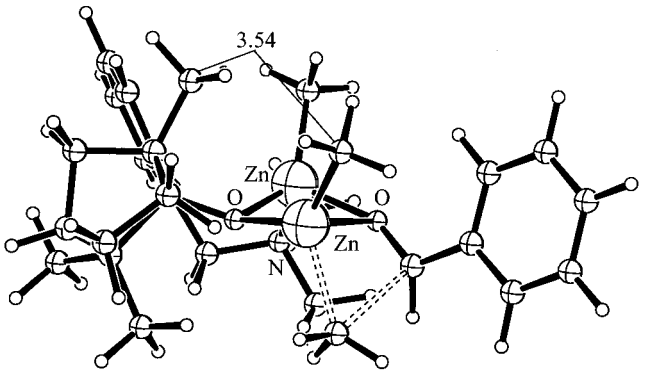

4-syn(*R*)

Figure 5. Transition structure geometries of **4**-anti(*S*) and **4**-syn(*R*); ONIOM(RHF/LanL2DZ:UFF). Distances are given in angstroms.

in **4**-syn(*R*) between the methyl group at C_1 of the bicyclo-[2.2.1]heptane moiety and the passive methylzinc group (C···C, 3.54 Å; Figure 5) can explain its discrimination relative to **4**-anti(*S*), which exhibits longer distances between the methyl group at C_1 of the bicyclo[2.2.1]-heptane moiety and the transferring, more remote methyl zinc unit (C···C, 4.20 Å; Figure 5). The higher experimental enantioselectivity of **4** relative to **3** (Table 1), however, is not reproduced by the model calculations.

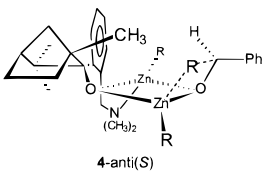

4-anti(*S*)

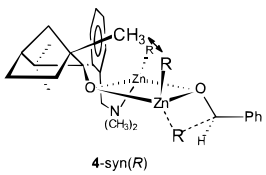

4-syn(*R*)

Conclusions

Experimentally it was found that both the directions and the degrees of enantioselectivity depend on the coordination group (D) of the fenchone-based ligands **1**,[9] **2**, **3**, and **4** in diethylzinc additions to benzaldehyde. Analyses of "anti" and "syn" μ-O transition structures (with di*methyl*zinc as model for di*ethyl*zinc) demonstrate how these different D groups effect the relative stabilities of the transitions structures and give rise to the experimental observations. For ligand **1**, repulsive interactions between the $N(CH_3)_2$ unit and the transferring alkylzinc group disfavor the **1**-syn(*S*) structure. The **1**-anti(*R*) transition structure is favored, which leads to the formation of the *R*-enantiomeric product. For ligands **2** and **3**, repulsive interactions between methyl groups at C_1 of the bicyclo[2.2.1]heptane moieties and passive methyl zinc groups disfavor **2**,**3**-anti(*R*) structures and favor the formation of the *S*-alcohol via **2**,**3**-syn(*S*) structures. The higher computed and observed enantioselectivity for **3** relative to **2** corresponds to closer contacts and more intense interactions in the structures of **3**. For ligand **4**, interactions between methyl groups at C_1 of the bicyclo-[2.2.1]heptane moieties and the passive methylzinc group in **4**-syn(*R*) favor the formation of the *S*-product via the **4**-anti(*S*) transition structure. Hence, interactions between alkyl groups at zinc and the ligand are essential factors for the mechanisms of enantioselection. This demonstrates possibilities for controlling enantioselectivity, e.g. by tuning of the ligands, in dialkylzinc additions to aldehydes.

Experimental Section

General Methods. All reactions were carried out under argon atmosphere using Schlenk-tube techniques. Solvents were dried by standard methods and distilled under argon prior to use.

Synthesis and Characterization of 2 (1*R*,2*R*,4*S*)-*exo*-(2-Methoxyphenyl)-1,3,3-trimethylbicyclo[2.2.1]heptan-2-ol.[17] A solution of *o*-lithioanisole[18] in TMEDA/hexanes was prepared from 0.15 mol of *n*-butyllithium (1.6 M, 94 mL) in hexanes, 0.15 mol of TMEDA (22.5 mL), and 0.15 mol of anisole (16.4 mL). (−)-Fenchone (0.15 mol, 24.1 mL) was added at 0 °C and the mixture was stirred for 5 h at 24 °C. Hydrolytic workup, washing, drying, and crystallization at 6 °C yielded a crude product, which was recrystallized from pentane. Colorless crystals of **2** were obtained (28.6 g, 0.11 mol, 70%). Mp: 69 °C. Calcd: C, 78.42; H, 9.29. Found: C, 78.38; H, 9.24. $[a]^{21}_D$: −90 (*c* 1.2, hexanes). ^{1}H NMR (200 MHz, $CDCl_3$) δ: 0.43 (3H, s), 1.00−1.90 (13H, m), 3.86 (3H, s), 6.79−7.53 (4H, m). ^{13}C NMR ($CDCl_3$) δ 18.24, 22.41, 24.67, 29.35, 33.40, 40.78, 44.76, 50.08, 52.50, 55.20, 85.37, 111.05, 119.76, 126.91, 128.87, 132.71, 157.82. IR (KBr, cm^{-1}) 3528, 3120, 3070, 2988, 2957, 2926, 2882, 2832. X-ray crystal data of **2**: four crystallographically unequivalent molecules of **2** appear in the asymmetric unit but exhibit very similar geometries; $C_{17}H_{24}O_2$; M = 260.36; space group *P*21; a = 20.137(4) Å; b = 7.532(4) Å; c = 22.148(5) Å; V = 3001.5(18) Å^3; Z = 8; T = 293(2) K; μ = 0.574; reflections total 4867; reflections observed ($>2\sigma(I)$) 3918; parameters refined 706; final R values, R_{obs} = 0.0455; wR_{all} = 0.1884; GOF_{all} = 1.080.

Synthesis and Characterization of 3 (1*R*,2*R*,4*S*)-*exo*-(2-*N*-Methylimidazolyl)-1,3,3-trimethylbicyclo[2.2.1]-heptan-2-ol. A solution of 2-lithium *N*-methylimidazole[18] in THF/hexanes was prepared from 0.15 mol of *n*-butyllithium (1.35 M, 107 mL) in hexanes, 50 mL of THF, and 0.15 mol of *N*-methylimidazole (12.0 mL) at −78 °C. (−)-Fenchone (0.15 mol, 24.1 mL) was added, the mixture was stirred for 1 h at −78 °C and then 3 h at 24 °C. Hydrolytic workup, washing, drying, and crystallization at 6 °C gave a crude product, which was recrystallized from diethyl ether, yielding colorless crystals of **3** (22.7 g, 0.097 mol, 65%). Mp: 133 °C. Calcd: C, 71.76; H, 9.46; N, 11.95. Found: C, 71.77; H, 9.46; N, 11.83. $[a]^{20}_D$:

(17) For the enantiomer of **2**, (1*S*,2*S*,4*R*)-*exo*-(2-methoxyphenyl)-1,3,3-trimethylbicyclo[2.2.1]heptan-2-ol, see: (a) Starling, S. M.; Vonwiller, S. C.; Reek, J. N. H. *J. Org. Chem.* **1998**, *63*, 2262. (b) Fry, J. L.; West, J. W. *J. Org. Chem.* **1981**, *46*, 2177.

(18) Brandsma, L.; Verkruijsse, H. Preparative *Polar Organometallic Chemistry*; Springer: Heidelberg, 1987.

−62 (*c* 2.7, EtOH). ^{1}H NMR (200 MHz, $CDCl_3$) δ: 0.47 (3H, s), 0.95−2.20 (13H, m), 3.74 (3H, s), 6.63 (1H, d), 6.78 (1H, d). ^{13}C NMR ($CDCl_3$) δ: 17.53, 22.74, 25.22, 27.57, 30.89, 35.88, 40.75, 45.99, 49.56, 54.14, 83.98, 121.33, 125.35, 150.07. IR (KBr, cm^{-1}) 3220, 3120, 3007, 2934, 2928, 2876. X-ray crystal data of **3**: $C_{14}H_{22}N_2O_1$; M = 234.34; space group $P61$; a = b = 12.7633(12) Å; c = 15.8762(14) Å; V = 2239.8(4) Å^3; Z = 6; T = 293(2) K; μ = 0.515; reflections total 1152; reflections observed (>2σ(I)) 977; parameters refined 160; final R values, R_{obs} = 0.0372; wR_{all} = 0.1052; GOF_{all} = 1.033.

Synthesis and Characterization of 4 (1*R*,2*R*,4*S*)-*exo*-(2-*N*,*N*-Dimethylbenzylamine)-1,3,3-trimethylbicyclo[2.2.1]-heptan-2-ol. A solution of 2-lithium *N*,*N*-dimethylbenzylamine[18] in hexanes was prepared from 0.15 mol of *n*-butyllithium (1.6 M, 94 mL) in hexanes and 0.15 mol of *N*,*N*-dimethylbenzylamine (22.5 mL) at 70 °C. (−)-Fenchone (0.15 mol, 24.1 mL) was added at 24 °C, the mixture was stirred for 3 h at 24 °C. Hydrolytic workup, washing, drying, and crystallization at 6 °C yielded a crude product, which was recrystallized from diethyl ether, yielding colorless crystals of **4** (34.5 g, 0.12 mol, 80%). Mp: 80 °C. Calcd: C, 79.39; H, 10.17; N, 4.87. Found: C, 79.32; H, 10.20; N, 4.83. [a]$^{23}_D$: −149 (*c* 1.0, hexanes). ^{1}H NMR (200 MHz, $CDCl_3$) δ: 0.43 (3H, s), 1.00−1.90 (13H, m), 2.24 (6H, s), 2.96 (1H, d), 4.01 (1H, d), 7.06−7.72 (4H, m). ^{13}C NMR ($CDCl_3$) δ: 18.50, 24.02, 24.46, 29.97, 34.20, 41.24, 44.14, 46.50, 50.69, 54.40, 65.29, 86.50, 125.33, 126.15, 130.43, 133.50, 137.00, 145.50, 175.50. IR (KBr, cm^{-1}) 3208, 3120, 3064, 3001, 2976, 2917, 2868, 2828, 2782. X-ray crystal data of **4**: $C_{19}H_{29}N_1O_1$; M = 287.18; space group $P21$; a = 8.869(2) Å, b = 9.068(2) Å; c = 10.741(1) Å; V = 862.8-(3) Å^3; Z = 2; T = 293(2) K; μ = 0.442; reflections total 1379; reflections observed (>2σ(I)) 1056; parameters refined 190; final R values, R_{obs} = 0.045; wR_{all} = 0.046; GOF_{all} = 1.488.

Catalyses. Catalyses with ligands **2**, **3**, and **4** were performed according to the following general procedure: 0.07 mmol (3 mol % with respect to benzaldehyde) of the ligand was treated with 3.3 mL (3 mmol) of diethylzinc in hexanes (0.9 M) at room temperature for 15 min. To this mixture was added 0.25 g (2.4 mmol) of benzaldehyde at the temperature specified for each ligand (Table 1). After the reaction time (24 h), the mixture was quenched with water and hydrolyzed with hydrochloric acid. The organic layer was separated, washed, neutralized ($NaHCO_3$), dried (Na_2SO_4) and 1-phenyl-1-propanol was distilled. The optical purity was measured by polarimetry and the enantiomeric excess was analyzed by chiral HPLC (Chiracel OB-H, 99.2:0.8 hexanes:*i*-PrOH, 25 °C, 254 nm, 1-phenyl-1-propanol:18.5 min (*S*), 25.6 min (*R*).

Computational Details. All transition structures were fully optimized without constraints using Morokuma's ONIOM[13] method implemented in GAUSSIAN98,[19] combining ab initio levels (RHF/LanL2DZ) with Rappe's universal force field (UFF).[14] Hydrogen atoms were used as link atoms between the two layers (RHF/LanL2DZ:UFF). All transition structures were analyzed by frequency computations and showed one imaginary frequency of the methyl transfer mode.

Acknowledgment. B.G. thanks the Fonds der Chemischen Industrie for a Liebig grant, the Alexander von Humboldt foundation for a Lynen scholarship, the Deutsche Forschungsgemeinschaft and the Research Pool Foundation (University Heidelberg) for financial support, the Degussa-Hüls AG for generous gifts of chemicals, and especially Prof. Dr. P. Hofmann for generous support at Heidelberg. We are grateful to Dr. S. Dapprich (Karlsruhe) for helpful discussions and to Priv. Doz. Dr. U. Kazmaier (Heidelberg) for providing a chiral HPLC column. We thank the National Institute of General Medical Sciences, National Institutes of Health, for support of this work in the U.S.A.

Supporting Information Available: Tables of X-ray structural data for compounds **2**−**4** and tables of energies and Cartesian coordinates of the computed transition structures. This material is available free of charge via the Internet at http://pubs.acs.org.

JO991070V

(19) Frisch, M. J.; Trucks, G. W.; Schlegel, H. B.; Scuseria, G. E.; Robb, M. A.; Cheeseman, J. R.; Zakrzewski, V. G.; Montgomery, Jr., J. A.; Stratmann, R. E.; Burant, J. C.; Dapprich, S.; Millam, J. M.; Daniels, A. D.; Kudin, K. N.; Strain, M. C.; Farkas, O.; Tomasi, J.; Barone, V.; Cossi, M.; Cammi, R.; Mennucci, B.; Pomelli, C.; Adamo, C.; Clifford, S.; Ochterski, J.; Petersson, G. A.; Ayala, P. Y.; Cui, Q.; Morokuma, K.; Malick, D. K.; Rabuck, A. D.; Raghavachari, K.; Foresman, J. B.; Cioslowski, J.; Ortiz, J. V.; Stefanov, B. B.; Liu, G.; Liashenko, A.; Piskorz, P.; Komaromi, I.; Gomperts, R.; Martin, R. L.; Fox, D. J.; Keith, T.; Al-Laham, M. A.; Peng, C. Y.; Nanayakkara, A.; Gonzalez, C.; Challacombe, M.; Gill, P. M. W.; Johnson, B.; Chen, W.; Wong, M. W.; Andres, J. L.; Gonzalez, C.; Head-Gordon, M.; Replogle, E. S.; Pople, J. A. Gaussian 98, Revision A.5, Gaussian, Inc., Pittsburgh, PA, 1998.

(20) Plots were generated with WinOrtep: Farrugia, L. J. *J. Appl. Crystallogr.* **1997**, 565.